

Nodal Spread of Squamous Cell Carcinoma of the Oral Cavity Detected with PET-Tyrosine, MRI and CT

Jan W. Braams, Jan Pruim, Peter G.J. Nikkels, Jan L.N. Roodenburg, Willem Vaalburg and Albert Vermeij
Departments of Oral and Maxillofacial Surgery, Pathology, Surgical Oncology and PET Center, Groningen University Hospital, Groningen, The Netherlands

The uptake of L-1-[¹¹C]-tyrosine (TYR) in cervical lymph nodes of eleven patients with squamous-cell carcinoma (SCC) of the oral cavity was studied with PET to detect lymphogenic metastases. **Methods:** The TYR-PET results were compared with clinical, MRI, CT, histopathologic findings and historical data of patients studied with FDG. Sensitivity, specificity, accuracy and the positive and negative predictive values were calculated. **Results:** TYR-PET had sensitivity of 83% and a specificity of 95%. In contrast, the sensitivity and specificity for MRI were 33% and 96%, respectively. The sensitivity and specificity for CT were 55% and 91%, respectively. TYR-PET results compared favorably with FDG. **Conclusion:** With TYR-PET, SCC metastases of the oral cavity can be visualized with high sensitivity and specificity. TYR-PET can be an additional tool for further evaluation of neck malignancies.

Key Words: PET; L-1-[¹¹C]-tyrosine; MRI; CT; head and neck cancer; metastases

J Nucl Med 1996; 37:897-901

The assessment of the presence of cervical lymph node metastases of squamous-cell carcinomas (SCCs) of the oral cavity in a "clinically negative neck" is difficult. Detecting such occult metastases is clinically important, since the extent of the treatment is determined by tumor size and the presence or absence of metastatic lymph nodes.

Available imaging techniques such as MRI, CT and US have improved tumor staging of the neck as compared to palpation. With these techniques, it is possible to monitor tumors and metastases by size and structural changes and not by metabolic activities. The overall error rate of assessing the presence or absence of cervical lymph node metastases by palpation is 20%–28%, error rate 7.5%–28% for CT and is 16% for MRI (1,2). Consequently, an imaging modality that can detect nodal metastases with high sensitivity and specificity is useful for accurate treatment planning of head and neck cancer.

An alternative way of cancer imaging is to use the physicochemical properties of tumor cells. For instance, it has been shown that malignant cells have an increased glucose consumption due to an increased glycolysis (3). Based on these findings, various investigators have applied 2-deoxy-2-[¹⁸F]fluoro-D-glucose (FDG) as a marker of tumor tissue in PET. Although FDG-PET imaging of SCC may be useful in detecting nodal metastases in the neck (4), it is hampered by high false-positive rates due to FDG accumulation in inflammatory tissues (5). We have found similar limitations (4).

As an alternative, some centers have started to use ¹¹C-labeled amino acids, mainly methyl-labeled ¹¹C-methionine. Lindholm et al. (6) studied L-[methyl-¹¹C]methionine (MET) uptake in patients with head and neck cancer and found that MET is useful in PET imaging of head and neck cancer.

Ishiwata et al. (7), however, found that MET visualized amino acid transport phenomenon rather than found protein synthesis rates. We used the carboxyl-labeled amino acid tyrosine, L-1-[¹¹C]-tyrosine (TYR) because it is possible to reflect the protein synthesis rate in cancer cells with TYR. So far, TYR has been successfully used in rats and humans to visualize different tumors and to quantitate protein synthesis rates (8,9).

The aim of this study was to investigate whether cervical nodal spreading of SCC of the oral cavity can be visualized with TYR-PET and to compare these results with the clinical, MRI, CT and histopathologic findings. Also, a comparison was made with historic data from a group of patients studied with FDG (4).

MATERIALS AND METHODS

Patients

Eleven patients (7 men, 4 women; mean age 62.3 yr) who underwent treatment of a SCC of the oral cavity were studied (Table 1). In all patients, there was an indication for a therapeutic or elective neck dissection. None of the patients received preoperative radiotherapy or chemotherapy. The study was approved by the Medical Ethics Committee of the University Hospital Groningen. Before entrance into the study, written informed consent was obtained from all patients. The characteristics of the 12 patients who had previous FDG studies have been previously published (4).

Staging of the tumor and its metastases was based on the International Union against Cancer (UICC, 1992) and American Joint Committee on Cancer (AJC, 1988) TNM classification. Histological typing of the primary tumor and metastases was performed according to the WHO (1978) classification (10).

Tracer Synthesis

Initially, L-1-[¹¹C]-tyrosine was produced through the isocyanide route as described by Bolster et al. (11) with a radiochemical purity of > 99% and a specific activity of > 3.7 GBq/μmole. To increase production yield at a later time, remote-controlled synthesis of non-carrier-added L-1-[¹¹C]-tyrosine through a microwave-induced Bücherer-strecker synthesis was developed.

PET

Studies were performed on a whole-body tomograph that acquires 31 planes across an axial length of 10.8 cm. The measured resolution of the system is 6 mm FWHM transaxially in the center of the field of view.

To prevent overlap of anatomical structures and head movements during the study, an individual foam-filled headmold was made. The method of fixation was standardized. The patient's head was positioned in the headmold so that the Frankfurter horizontal plane (defined as an imaginary line between the external ostium of the ear and the lower orbital rim) made a 110° angle with the horizontal bed position. This position was reached by requesting

Received Apr. 27, 1995; revision accepted Oct. 8, 1995.

For correspondence or reprints contact: J.W. Braams, DDS, Department of Oral and Maxillofacial Surgery, Groningen University Hospital, P.O. Box 30.001, 9700 RB Groningen, The Netherlands.

TABLE 1
Assessment of Lymph Node Metastases of SCCs of the Oral Cavity

Patient no.	Sex	Age (yr)	Tumor	Metastases*				Neck treatment†	
			Stage, location‡ R/L	Clinical R/L	PET R/L	MRI R/L	CT R/L	Hist. R/L	R/L
1	M	73	T2N0, floor mouth R	-/-	+/+/+	-/-		++/-	SOND/-
2	F	70	T4N1, retromol.trig.R	+/-	+/+/-	+/+/-		-/-	MRND/-
3	M	53	T4N2, floor mouth RL	+/+/+	+/+/+		+/+/+	+/+/+	MRND/MRND
4	F	73	T4N0, lower gum R	-/-	+/+	-/+		-/-	SOND/SOND
5	M	59	T1N0, floor mouth L	-/-	-/-	-/-		-/-	-/SOND
6	M	66	T4N2a, floor mouth R	+/+/-	+/+/-	+/+/-		+/+/-	MRND/-
7	F	69	T2N0, oral cheek L	-/-	-/-		-/-	-/-	-/MRND
8	M	64	T4N2b, floor mouth R	+/+/-	-/-		+/+/-	-/-	MRND/-
9	F	56	T4N2b, floor mouth R	+/+/-	+/+/+		-/-	+/+/-	SOND/SOND
10	M	46	T4N2b, floor mouth L	-/++	-/++	+/+/+		-/++	-/MRND
11	M	56	T4N0, floor mouth L	-/-	-/-	-/+		-/++	SOND/MRND

*Clinical, PET, MRI and histopathological staging of both sides of the neck (- = no suspicious nodes, + = one suspicious node, ++ = two or more suspicious nodes).

†Neck treatment that has occurred (- = no treatment, SOND = supraomohyoid neck dissection, MRND = modified radical neck dissection).

‡T- and N-stage according to the UICC (1992) and AJCC (1988) classifications of the primary tumor and location. Retromol.trig. = retromolar trigone.

the patient to stretch the neck by moving the head backwards. For anatomical orientation, small radioactive markers were placed on the tip of the chin, the mandibular angles, the midline of the clavicles and the sternal notch.

Two transmission scans of 15 min each were obtained: one cranial and one caudal. The total distance was 21 cm. After transmission scanning, TYR (370 MBq) was injected into a peripheral vein of the arm and the markers were placed. Data acquisition was started 20 min postinjection. To cover the whole neck, 10-min cranial and caudal scans were made in reverse order as compared to the transmission scans.

Any visually positive hot spot on each emission scan was considered to be a metastatic hot spot. This procedure was identical to the FDG procedure published earlier (4), but left and right symmetrically located hot spots in the sagittal planes were assumed to be the salivary glands. Standardized uptake values were not calculated due to the poor results in the FDG study.

MRI

Seven patients underwent MRI. T1- (TR = 650 msec, TE = 20 msec) and T2- (TR = 2000 msec, TE = 50–100 msec) weighted pulse sequences were obtained. A head coil was used to obtain axial and coronal slices with a slice thickness varying between 3–5 mm. We used the following radiologic criteria (2) to assess cervical metastases in patients with a primary SCC:

1. Nodes with a minimal axial diameter of 11 mm or more in the subdiaphragic region and 10 mm or more in the other lymph node-bearing regions were considered metastatic.
2. Groups of three or more lymph nodes of 9 or 10 mm in the subdiaphragic region and of 8 or 9 mm in the other lymph node drainage regions of the tumor were considered metastatic.
3. All nodes that showed irregular enhancement on MRI and were surrounded by a rim of enhancing viable tumor or lymph node tissue were considered metastatic.

CT

Four patients underwent CT instead of MRI. Axial and coronal slices were made with a slice thickness varying between 5–10 mm. Intravenous contrast medium was administered to all patients. The criteria for delineating a lymph node metastasis were the same as those used for MRI.

Histopathology

Shortly after the PET, MRI or CT studies, radical surgery of the primary tumor and selective or modified radical neck dissection was performed (median time interval between the studies and the surgical procedure was 4.5 days). The removed specimen was stretched out on a polystyrene pad and the coordinates were marked immediately after removal by the surgeon using colored pins. From the specimen, all lymph nodes were studied individually using H&E staining. From each lymph node, the largest diameter was measured for lymph nodes with a diameter of 2 cm or more, several samples were examined.

Data Analysis

Applying standard manufacturer software, the transversal PET images were individually reoriented to sagittal and coronal planes to obtain a better view of the lymph nodes, especially of those lying in clusters. The images were analyzed visually by two observers at the same time. Disagreements were solved by consensus. The number and location of the positive nodes were assessed.

A similar approach was done for the MRI and CT. The PET, MRI and CT observers were unaware of each other's results and of the histopathology. Sensitivity, specificity, positive and negative predictive values and accuracy were calculated for the lymph node metastases detected by PET, MRI and CT against histopathology. Finally, the TYR-PET results were compared with those obtained from an earlier FDG-PET study (4).

RESULTS

Histopathology of the resected neck specimens depicted a total of 287 lymph nodes, 24 of which were metastatic. PET depicted 32 positive lymph nodes (Fig. 1). Twenty of the 24 histopathologic metastatic lymph nodes were visualized with PET. The 12 other lymph nodes that showed positive with PET were normal on histopathological examination (Table 2). The smallest metastatic lymph node detected was 0.5 cm. Four metastatic lymph nodes were not detected with TYR-PET (0.4–1.2 cm).

MRI depicted 155 lymph nodes, 11 of which were positive lymph nodes. When compared with the histopathological results, five nodes were metastatic and six lymph nodes were normal. In the resected specimens, 15 metastatic lymph nodes were found after histopathological examination. Obviously,

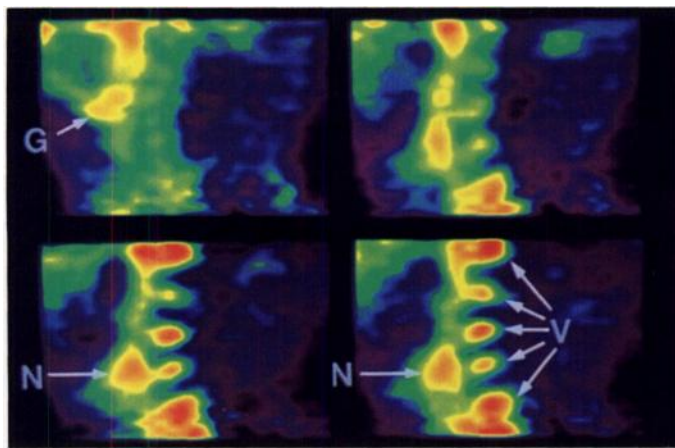


FIGURE 1. Example of sagittally reoriented PET images of a metastatic lymph node in the midjugulum (N) of a patient with a T2N1 carcinoma of the oral cavity. There is also high uptake in the submandibular gland (G) and in the bone marrow of the cervical vertebrae (V).

MRI missed 10 metastatic lymph nodes, which were between 0.5–1.5 cm (Table 2).

Finally, for CT (132 lymph nodes were evaluated), of the nine histologically proven metastatic nodes, CT detected five. Ten lymph nodes that were positive on CT were normal on histopathological examination (Table 2). The metastatic lymph nodes missed by CT varied in size from 0.8 to 3.0 cm. The smallest metastatic lymph node detected with MRI or CT was 1.0 cm.

Sensitivity, specificity, positive and negative predictive values and accuracy were calculated for all three diagnostic imaging modalities (Table 3).

DISCUSSION

The presence of cervical lymph node metastases in SCC of the oral cavity will often change the extent of surgical treatment. For instance, at our institution a T1N0 oral cavity SCC is treated with local resection of the tumor alone and a “watchful, waiting policy” is used for the neck. If metastatic lymph nodes are found, the treatment consists of resection of the primary tumor and a supraomohyoid or modified radical neck dissection. In case the primary tumor is stage T2 or more and no cervical lymph nodes are clinically evident (or evident by imaging), elective neck dissection is indicated. Thus, a reliable estimation of the presence of metastatic lymph nodes is needed to prevent overtreatment.

So far, the surgeon largely depends on palpation to assess the presence of metastatic lymph nodes. Several clinicians have sought more modern techniques that will allow better assess-

TABLE 2
PET, MRI, CT and Histopathology Results

Modality	Histopathology		Total
	Metastatic	Normal	
PET positive	20	12	32
PET negative	4	251	255
Total	24	263	287
MRI positive	5	6	11
MRI negative	10	134	144
Total	15	140	155
CT positive	5	10	15
CT negative	4	113	117
Total	9	123	132

TABLE 3

Sensitivity, Specificity, Accuracy and Positive and Negative Predictive Values for TYR-PET, MRI, CT and FDG-PET*

	TYR-PET (%)	MRI (%)	CT (%)	FDG-PET (%)
Sensitivity	83	33	55	91
Specificity	95	96	91	88
Accuracy	95	90	89	88
PPV	63	45	33	48
NPV	98	93	97	99

*Results of previously published study (4).

PPV = positive predictive value; NPV = negative predictive value.

ment of the presence of cervical metastatic lymph nodes. Van den Brekel et al. (12) described the assessment of lymph node metastasis in the neck with different imaging modalities. They concluded that CT and MRI are superior to palpation in detecting or excluding metastatic neck disease. They also concluded that although it is possible to reliably upstage more than half of the clinically negative necks with CT, MRI and US, US-guided fine needle aspiration cytology (FNAC) is the most sensitive, specific and accurate technique to detect or exclude the presence of metastases preoperatively. However, with US-guided FNAC, no standardized permanent document is obtained and the accuracy of the technique fully depends on the examiner. Finally, Van den Brekel et al. concluded that patients with undoubtedly palpatory evidence of unilateral mobile metastases on the side of the primary tumor well confined to one side, or patients with bilateral palpatory mobile metastases, do not need US-guided FNAC. Also patients who need radiologic staging (CT or MRI) for their primary tumor need no US-guided FNAC of the neck, if the neck is included in the imaging. The reliability of CT and MRI, however, is doubtful and largely depends on the experience of the investigator.

We have explored the possibilities of PET for the detection of metastatic lymph nodes. The main advantage of PET over the other imaging techniques is that it evaluates metabolism rather than structure. In an earlier investigation, we studied the possibilities of the widely used tracer FDG (4).

Our previous results showed that PET-FDG is a good indicator of the presence of metastatic lymph nodes. However, several false-positive results were encountered due to the fact that reactive lymph nodes also yield a positive signal. Even with the standardized uptake values of the true-positive and false-positive lymph nodes, no differentiation could be made. Indeed, Kubota et al. (13) have shown that leukocytes also have high glucose consumption and consequently high FDG uptake. A main quest for PET research still is to find a way to differentiate between cancerous cells and inflammatory cells.

To circumvent this problem, we studied the possibilities of TYR as a tracer. This tracer shows high incorporation rates into proteins while, when catabolized, the ^{11}C -label leaves the body as $^{11}\text{CO}_2$ in an earlier step. Our experiences with TYR in other types of cancer are promising (9,11). TYR-PET compared favorably with CT and MRI in terms of sensitivity, accuracy and positive predictive values. Compared with the FDG results from our previous paper (4), TYR has higher specificity, accuracy and positive predictive values. Therefore, we believe that TYR-PET appears to be the most reliable technique so far to assess the presence of metastatic lymph nodes in the necks of patients with SCC of the oral cavity.

Despite these favorable results, there were more false-negatives ($n = 5$) than in our earlier FDG study. One metastatic

lymph node was in a cluster of five interconnected metastatic lymph nodes. Another metastatic lymph node was in close proximity to the primary tumor and the submandibular gland. Despite its size of 1.2 cm, this metastasis was not detected. The remaining two undetected metastatic lymph nodes were 0.4 cm in size (Table 2).

The fact that one metastatic lymph node in a cluster of five interconnected metastases was not found, is probably due to the high uptake of TYR from the neighboring positive lymph nodes and the partial volume effect. Another explanation could be that no delineation is possible from that cluster of metastatic lymph nodes due to the camera resolution used. However, this negative PET result did not affect the clinical management of the patient.

Similarly, one metastatic lymph node was not visualized because of the high activity from the primary tumor and the submandibular gland, which were closely related to each other. The active uptake of TYR by the salivary glands may be a severe drawback of the TYR-PET technique.

Finally, TYR-PET did not detect two small (0.4 cm) metastatic lymph nodes. The size of these metastatic nodes suggests that size is a factor in undetected nodes. Indeed, 0.4 cm is at the lower end of the resolution of current PET cameras. Newer systems have a slightly better resolution, but there is a physical limitation of about 0.3 cm. Consequently, PET will never be suitable for detecting microscopic disease, although much smaller metastatic lymph nodes can be better identified than with MRI or CT. It can also be argued that the metastatic lymph nodes could not be delineated from the surrounding tissue because of a low protein synthesis rate. Minn et al. (14), in their study of a specially collimated gamma camera and FDG, suggested that low glycolytic activity could be the explanation for undetected metastases of a breast tumor. An extrapolation of this suggestion could explain that it is also possible to have a low protein synthesis rate.

The smallest lymph node detected by TYR-PET was 0.5 cm, whereas the smallest detected metastatic lymph node with MRI and CT was 1.0 cm. This latter finding should be attributed to the radiologic criteria used. Van den Brekel et al. (2) consider 9–10 mm in the subdiaphragic region and 10–11 mm in the other lymph node drainage regions as the critical size to differentiate between metastases or reactive lymph nodes. Consequently, specificity of this technique is increased at the cost of lower sensitivity, since smaller lymph nodes are excluded by definition.

The number of false-positive lymph nodes with TYR-PET was relatively high: 12 lymph nodes. The origin of the positive signal is yet unclear, since all nodes were normal on histological examination. There were no reactive changes in these false-positive lymph nodes. Leskinen-Kallio et al. (15) reported on the uptake of amino acids in inflammatory processes. They found that MET accumulated slightly in a breast abscess (15). Lindholm et al. (6) also described the uptake of MET in inflammatory processes. FDG uptake in inflammatory tissues has been reported by other authors. Although histology gave no evidence of inflammatory processes yielding a positive signal, we have to realize that the advantage of ^{11}C -labeled amino acids over FDG is probably not a principal difference because it is derived from a small population of patients. A larger patient population should be studied to confirm this.

In all patients we found that TYR accumulates markedly in the sublingual, submandibular and/or parotid glands and sometimes in bone marrow. This high uptake in the salivary glands impairs the analysis of PET images, especially when the primary tumor or metastases are localized close to these structures. The submandibular lymph nodes are one of the first

nodal echelons which will be infested with micrometastases and are therefore difficult to detect. Lindholm et al. (6) described this phenomenon with MET, but they mentioned that these hot salivary glands could be landmarks to make it easier to localize the primary tumor in a PET image. We believe that placement of markers on earlier defined structures is preferable to landmarks in the field of view.

For clinical PET studies, FDG and TYR are two reliable tracers suitable for the detection of lymph node metastasis of SCC of the oral cavity. The higher sensitivity and predictive value of a negative test is an advantage of FDG-PET over TYR-PET. The relatively high uptake in reactive tissue, however, is a severe drawback of FDG. The specificity, accuracy and positive predictive value make TYR-PET more favorable, although the TYR uptake in the salivary glands impairs image analysis.

Consequently, we slightly prefer FDG-PET in patients with clinically negative neck metastases. Patients with palpable lymph nodes in the neck should be scanned with TYR-PET.

PET imaging, as applied in this and the previous study, is rather cumbersome for the patient. It is time-consuming and requires that the patient lie quietly for a long time. Most of the time is needed to obtain two transmission scans (total time 1 hr), and, including the emission scans, the procedure takes more than 1.5 hr. To reduce this time frame, a less time-consuming technique is needed. A few years ago, Guerrero et al. (16) and Dahlbom et al. (17) introduced whole-body scanning software for ECAT cameras (16,17). In this software, no transmission scanning is applied, and the scan time per bed position is often less than 10 min. We are currently investigating whether whole-body scanning for the head and neck region yields results similar to those in this study.

CONCLUSION

A metabolic imaging technique as TYR-PET is an important diagnostic tool in the assessment of the presence of metastatic lymph nodes in patients with SCC of the oral cavity. The technique is superior to imaging techniques based on structural alterations such as CT and MRI. The high specificity, accuracy and predictive values make TYR-PET suitable for further evaluation of neck metastases. The high sensitivity and negative predictive value makes FDG-PET preferable for evaluation of neck metastases with stage N_0 .

REFERENCES

1. Van den Brekel MWM, Castelijns JA, Croll GA, et al. Magnetic resonance imaging versus palpation of cervical lymph node metastases. *Arch Otolaryngol Head Neck Surg* 1991;117:666–673.
2. Van den Brekel MWM, Stel HV, Castelijns JA, et al. Cervical lymph node metastasis: assessment of radiologic criteria. *Radiology* 1990;177:379–384.
3. Warburg O. *The metabolism of tumors*. London: Arnold Constable; 1930:75–327.
4. Braams JW, Pruijm J, Freling NJM, et al. Detection of lymph node metastases of squamous cell cancer of the head and neck with PET-FDG and MRI. *J Nucl Med* 1995;2:211–216.
5. Kubota R, Yamada S, Kubota K, Ishiwata K, Tamahashi N, Ido T. Intratumoral distribution of fluorine-18-fluorodeoxyglucose in vivo: high accumulation in macrophages and granulation tissues studied by microautoradiography. *J Nucl Med* 1992; 33:1972–1980.
6. Lindholm P, Leskinen-Kallio S, Minn H, et al. Comparison of fluorine-18-fluorodeoxyglucose and carbon-11-methionine in head and neck cancer. *J Nucl Med* 1993;34: 1711–1716.
7. Ishiwata K, Kubota K, Murakami M, et al. Re-evaluation of amino acid-pet studies: can the protein synthesis rates in the brain and tumor tissues be measured in vivo? *J Nucl Med* 1993;34:1936–1943.
8. Daemen BJG, Elsinga PH, Paans AMJ, Wieringa AR, Konings AWT, Vaalburg W. Radiation-induced inhibition of tumor growth as monitored by PET using L-1-[^{11}C]-tyrosine and ^{18}F -fluoride-oxyglucose. *J Nucl Med* 1992;33:373–379.
9. Daemen BJG, Zwertbroek R, Elsinga PH, Paans AMJ, Doorenbos H, Vaalburg W. PET studies with L-1-[^{11}C]-tyrosine, L-[methyl- ^{11}C]methionine and ^{18}F FDG in prolactinomas in relation to bromocryptine treatment. *Eur J Nucl Med* 1991;18:453–460.
10. Shanmugaratnam K, Sobin LH. *Histological typing of upper respiratory tract tumors*. Geneva: World Health Organization, 1978.

11. Bolster JM, Vaalburg W, Paans A, et al. Carbon-11 labeled tyrosine to study tumor metabolism by positron emission tomography (PET). *Eur J Nucl Med* 1986;12:321-324.
12. Van den Brekel MWM. Assessment of lymph node metastases in the neck. Thesis, Free University Amsterdam, Utrecht: Elinkwijk 1992.
13. Kubota R, Yamada S, Kubota K, Ishiwata K, Ido T. Microautoradiographic study of ¹⁸F-FDG: high accumulation in granulation tissues and phagocytes in mouse tumor tissue in vivo. *J Nucl Med* 1992;33:840-841.
14. Minn H, Soini I. Fluorine-18-fluorodeoxyglucose scintigraphy in diagnosis and follow-up of treatment in advanced breast cancer. *Eur J Nucl Med* 1989;15:61-66.
15. Leskinen-Kallio S, Nägren K, Lehtikoinen P, Ruotsalainen U, Joensuu H. Uptake of ¹¹C-methionine in breast cancer studied by PET: an association with the size of S-phase fraction. *Br J Cancer* 1991;64:1121-1124.
16. Guerrero TM, Hoffman EJ, Dahlbom M, Cutler PD, Hawkins RA, Phelps ME. Characterization of a whole-body imaging technique for PET. *IEEE Trans Nucl Sci* 1990;37:676-680.
17. Dahlbom M, Hoffman EJ, Hoh CK, et al. Whole-body positron emission tomography: part 1. Methods and performance characteristics. *J Nucl Med* 1992;33:1191-1199.

Technetium-99m-Sestamibi Scintigraphy Compared with Thallium-201 in Evaluation of Thyroid Tumors

Hiroshi Nakahara, Shiro Noguchi, Nobuo Murakami, Hiroaki Hoshi, Seishi Jinnouchi, Shigeki Nagamachi, Takashi Ohnishi, Shigemi Futami, Leo G. Flores II and Katsushi Watanabe

Noguchi Thyroid Clinic and Hospital Foundation, Beppu, Oita; and Department of Radiology, Miyazaki Medical College, Miyazaki, Japan

Technetium-99m methoxyisobutylisonitrile (MIBI) is a myocardial perfusion imaging agent that has been reported to effectively localize in various tumors (e.g., lung and thyroid carcinomas and osteogenic sarcoma). To determine its usefulness in thyroid tumors, we compared ^{99m}Tc-MIBI with ²⁰¹Tl imaging. **Method:** We evaluated 25 patients with thyroid tumors (papillary carcinoma in 11, follicular carcinoma in 2, follicular adenoma in 7, adenomatous goiter in 5). Fifteen metastatic lesions from differentiated thyroid carcinomas were also evaluated. Early (10 min after injection) and delayed images (120 min after injection) were obtained for both ^{99m}Tc-MIBI and ²⁰¹Tl scintigraphy. **Results:** The early images showed very similar findings for both ^{99m}Tc-MIBI and ²⁰¹Tl. However, the delayed images showed that malignant tumors tended to retain more tracer agent than benign nodules. Marked retention was in 61.5% (8 of 13) of ²⁰¹Tl images and 53.8% (7 of 13) of ^{99m}Tc-MIBI images. For metastatic lesions from thyroid carcinomas, the findings for ^{99m}Tc-MIBI imaging were nearly identical to those for ²⁰¹Tl imaging. A slight difference in clarity was seen that may have been due to the effect of the ^{99m}Tc. **Conclusion:** Although ^{99m}Tc-MIBI scintigraphy does not have particularly good results in differentiating malignant from benign thyroid tumors, it may be useful in evaluating metastases or predicting recurrence because of its better imaging characteristics.

Key Words: technetium-99m-sestamibi; thallium-201; thyroid tumors

J Nucl Med 1996; 37:901-904

Technetium-99m-methoxyisobutylisonitrile (MIBI) was introduced as a myocardial perfusion agent in 1989 (1,2). Like ²⁰¹Tl, ^{99m}Tc-MIBI has been reported to accumulate in benign and malignant lesions, such as lung (3,4), brain (5,6) and parathyroid tumors (7,8) and bone lesions (9).

In thyroid tumors, ²⁰¹Tl scintigraphy has been used to differentiate benign from malignant nodules (10-12) and to locate metastatic or recurrent lesions in follow-up studies (13-15). Delayed scanning was reported to be useful in differentiating malignant from benign tumors, but the results were not very satisfactory.

Recently, Maublant et al. (16) reported that accumulation of ^{99m}Tc-MIBI was more useful in distinguishing normal from malignant cells than ²⁰¹Tl in an in vitro study. In the present

report, we evaluate the usefulness of ^{99m}Tc-MIBI in differentiating malignancies in thyroid tumors and detecting metastatic or recurrent thyroid cancers.

MATERIALS AND METHODS

We studied 25 patients with primary thyroid tumor (21 women, 4 men; mean age 53.3 yr, range 29-75 yr) and 15 with metastatic or recurrent lesions from thyroid cancer (11 women, 4 men; mean age 58.8 yr, range 30-78 yr). Of the 25 patients with primary thyroid tumors, papillary carcinoma occurred in 11, follicular carcinoma in 2, follicular adenoma in 7 and adenomatous goiter in 5. In these patients, all but one tumor consisted mainly of a solid mass; the remaining adenomatous goiter had had small cystic components. Of the 15 patients with metastatic lesions from thyroid cancer, papillary carcinoma occurred in 13 (10 from the lymph nodes, 3 from the lungs) follicular carcinoma in 2 (both from bone).

All patients underwent both ^{99m}Tc-MIBI and ²⁰¹Tl scintigraphy within 5 days. The ^{99m}Tc-MIBI was prepared by adding 740 MBq of [^{99m}Tc]pertechnetate in 5 ml saline solution to a freeze-dried kit. In the 25 patients with primary thyroid tumor, 74 MBq ²⁰¹Tl was injected, and 185 MBq ^{99m}Tc-MIBI was administered intravenously. In the 15 patients with metastatic lesions, 111 MBq ²⁰¹Tl was injected, and 740 MBq ^{99m}Tc-MIBI was administered intravenously. At follow-up study, thyroid suppression therapy (thyroxine medication) was not stopped before the studies, and ¹³¹I studies were not performed in all patients.

Static images were obtained 10 min (early image) and 120 min (delayed image) after injection in patients with primary thyroid tumors. Whole-body and static images (early and delayed images) were obtained in patients with metastatic lesions. Imaging was performed with a gamma camera with a high-resolution collimator.

Accumulation of both ^{99m}Tc-MIBI and ²⁰¹Tl in primary thyroid tumors was classified as high (uptake in tumor was higher than that in normal thyroid tissue); iso (uptake in tumor was almost equal to that of normal thyroid tissue); or low (uptake in tumor was lower than that in normal thyroid tissue).

A semiquantitative method for assessing uptake was used, whereby uptake was measured in rectangular (10 mm × 10 mm) regions of interest (ROIs) over tumor and normal thyroid tissue. Tumor uptake of ^{99m}Tc-MIBI and ²⁰¹Tl was expressed as the

Received Jul. 14, 1995; revision accepted Dec. 13, 1995.
For correspondence or reprints contact: Hiroshi Nakahara, MD, Miyazaki Medical College, 5200 Ohaza Kihara, Kiyotake, Miyazaki, Japan 889-16.